# Analysis of Composite-Reinforced Cutouts and Cracks

RICHARD A. MITCHELL,* RUTH M. WOOLLEY,† AND DANIEL J. CHWIRUT‡
*National Bureau of Standards, Washington, D.C.*

**Finite element computer analyses of the reinforcement of cutouts and cracks in metal sheet, by bonded overlays of composite material, are described. The analyses articulate the separate responses of the sheet, the overlays, and the adhesive. Contour plots of computed stress and strain fields are automatically generated by the computer programs. Strains measured on the surfaces of several reinforced-sheet tensile specimens were, for the most part, in good agreement with strains predicted by the analyses. Qualitative correlations between certain failure modes observed in the test specimens and the stress distributions given by finite element analysis are apparent. The same analytical approach is currently being used to study weld/bond and fastener/bond joints, and it could be used to study other problems such as hole repair in metal or composite sheet and embedded defects in laminar material.**

## Introduction

A BONDED overlay of high-strength, high-stiffness composite material offers an efficient means of achieving local reinforcement of cutouts and cracks in metal sheet. This concept can be used in the design of new structures, or it can be used to strengthen existing structures. Where a crack is anticipated, on the basis of stress analysis or service experience, a composite overlay can be used to reduce the stresses that might otherwise initiate a fatigue crack. Where a crack already exists, a composite overlay can be used to bridge across the crack and stop or retard its growth.

The primary objectives of the work reported here were to develop methods of analysis of composite-reinforced cutouts and cracks and to demonstrate the validity of the analyses by laboratory testing. Finite element computer programs were developed for the study of three general configurations: 1) a sheet with a reinforced cutout, 2) a sheet with a reinforced cutout with 2 symmetrical transverse cracks within the sheet radiating away from the cutout edge, and 3) a sheet with a reinforced transverse crack. The same programs are also suitable for the analysis of adhesively bonded lap joints. Computer output in the form of contour plots of stress and strain fields throughout each of the components of the bonded system enables one to visualize the interactions between the sheet, the overlays, and the adhesive. The contour plots can also indicate the presence of a stress condition that might initiate or drive a crack or a debond. This analysis was developed independently of other finite element approaches that have been reported[1-3] for application to similar problems, and no attempt has been made to compare the efficiency of this analysis with the other methods.

## Finite Element Analyses

Separate finite element programs were developed for the planform analysis and the longitudinal cross-section analysis of a broad class of reinforced configurations. The analyses are formulated to articulate the separate responses of the metal sheet, the composite overlays, and the adhesive layers. Such special features as unreinforced-polymer cushions, tapers, and debonded regions are described explicitly. Effective orthotropic material constants of angle-ply composites are computed by transformation and integration. Although the basic finite element formulation is linear, the computer programs permit nonlinear shear deformation and progressive debonding to be approximated by a series of stepwise-linear solutions.

### Planform Analysis

Figure 1 shows a representative network of triangular finite elements as might be used in a planform analysis of a reinforced cutout. Symmetry is assumed about the horizontal ($x$) and vertical ($y$) axes of the cutout and, therefore, only one quadrant is analyzed. The sheet and the overlay are each divided into separate networks of triangular, constant strain, plane stress elements that are connected to adjacent elements of the same adherend only at common nodal points. Within the bonded-overlay region the triangular networks of the 2 adherends are congruent, and the 2 networks are coupled together by an array of special shear-stiffness elements linking conjugate pairs of nodal points. External normal and shear loads are assumed to act at the edge of the sheet and only in the midplane of the sheet. Out-of-plane deflections are ignored.

Stiffness computations for the triangular finite elements are formulated in terms of 4 independent, orthotropic material constants, as defined by Ashton, et al.[4] for two-dimensional stress states. In general, a composite overlay can consist of several laminas, each having an arbitrary orientation of principal orthogonal material axes. The orthotropic stress-strain properties of each lamina are first transformed to the axes $x$, $y$;

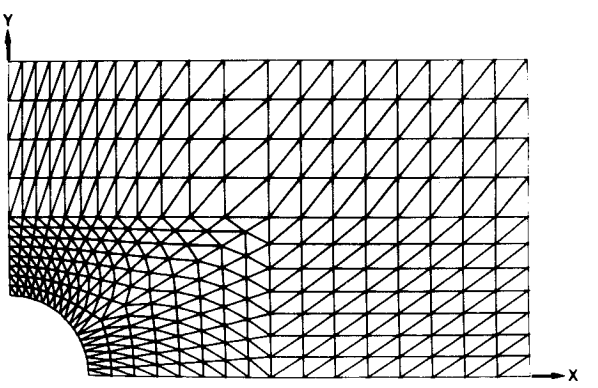


**Fig. 1 Finite element mesh for planform analysis of a reinforced cutout.**

Presented as Paper 74-377 at the AIAA/ASME/SAE 15th Structures, Structural Dynamics and Materials Conference, Las Vegas, Nevada, April 17–19, 1974; submitted April 25, 1974; revision received December 6, 1974. This work was done at the National Bureau of Standards with partial support by NASA Langley Research Center, Hampton, Virginia. Not subject to copyright. The following valuable contributions to this work are gratefully acknowledged: technical review and consultation, L. Mordfin; computer programing, S. M. Baker; specimen fabrication, R. L. Breeden; instrumentation, R. E. Snyder.

Index categories: Structural Static Analysis; Structural Composite Materials (including Coatings).

* Research Structural Engineer, Engineering Mechanics Section.
† Mathematician, Engineering Mechanics Section.
‡ Mechanical Engineer, Engineering Mechanics Section.

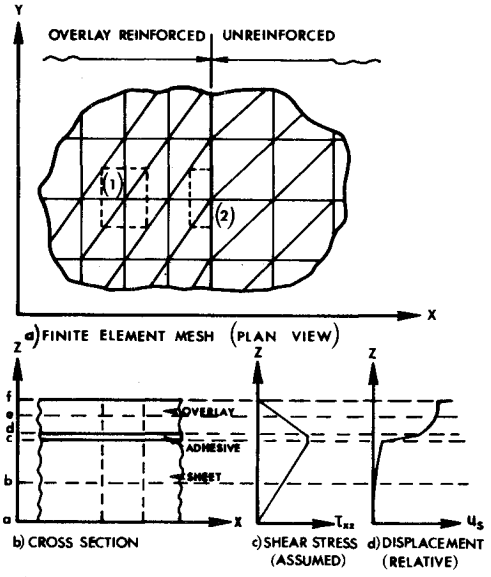


**Fig. 2 Schematic basis for shear-stiffness element.**

then the effective (weighted average) orthotropic properties are computed for each finite element by integrating through the thicknesses of the individual laminas at the centroid of the triangular element. The direct stiffness matrix of a triangular element $[k]$, which relates the 6 components of force $\{f\}$ acting at the nodal points to the 6 components of nodal point displacement $\{w\}$ by the expression

$$\{f\} = [k]\{w\} \tag{1}$$

is computed in the usual way. See, for example, Zienkiewicz.[5]

A different formulation is required for computation of the special shear-stiffness elements that couple conjugate pairs of nodal points in the 2 adherends. Figures 2a and 2b show, respectively, schematic plan and cross-section views of a region of an overlay-reinforced sheet. In Fig. 2b the $x$ axis is a line of symmetry in the doubly reinforced case; it is a free boundary in the singly reinforced case. In the shear-stiffness element formulation the interlaminar shear stress is assumed to vary as shown in Fig. 2c. That is, the shear stress is assumed to have a uniform maximum value at the adhesive layer ($c$ to $d$) and to decrease uniformly to zero at a free surface ($a$ or $f$) or at a plane of symmetry ($a$). The area of a shear-stiffness element in the $x$-$y$ plane is equal to $\frac{1}{3}$ of the sum of the bonded triangular areas meeting at an overlay nodal point. For example, the shear-stiffness element areas for nodal points 1 and 2 in Fig. 2a are equal to the areas within the dashed rectangles. The specific shapes of the shear-stiffness elements, in plan, are not defined in the analysis.

The nodal point stiffness matrix for a shear-stiffness element $[k_s]$ relates the 2 components of shear force $\{f_s\}$ acting in the adhesive layer to the 2 components of relative displacement of the overlay with respect to the sheet $\{w_s\}$ by the expression

$$\begin{Bmatrix} f_{sx} \\ f_{sy} \end{Bmatrix} = \begin{bmatrix} k_{sx} & 0 \\ 0 & k_{sy} \end{bmatrix} \begin{Bmatrix} u_s \\ v_s \end{Bmatrix} \tag{2}$$

or

$$\{f_s\} = [k_s]\{w_s\} \tag{3}$$

in which $u_s$ and $v_s$ are, respectively, the $x$ and $y$ components of the difference in displacement of the midplanes of the overlay and the sheet. It is assumed that the shear moduli are uniform within the sheet, within the adhesive, and within the overlay, and that each shear-stiffness element is deformed in pure shear. With these assumptions, the relative displacement within a shear-stiffness element can be approximated by an integral of the form (see Fig. 2d)

$$(u_s)_{me} = \int_m^c \frac{\tau_{xz}}{G_s} dz + \int_c^d \frac{\tau_{xz}}{G_a} dz + \int_d^e \frac{\tau_{xz}}{G_o} dz \tag{4}$$

in which $m = a$ in the case of a doubly reinforced sheet; $m = b$ in the case of a singly reinforced sheet; $(u_s)_{me}$ = difference between $x$ components of displacement at points $e$ and $m$ (point $a$ or $b$ in Fig. 2b); and $G_s$, $G_a$, and $G_o$ are, respectively, the shear moduli of the sheet, the adhesive, and the overlay. In the doubly-reinforced case, integration of Eq. (4) between points $a$ and $e$ and substitution into Eq. (2) gives the shear-stiffness coefficient

$$k_{sx} = \left( A_s \Big/ \frac{1}{2}\frac{t_s}{G_s} + \frac{t_a}{G_a} + \frac{3}{8}\frac{t_o}{G_o} \right) = k_{sy} \tag{5}$$

in which $A_s$ = the area of the shear-stiffness element in the $x$-$y$ plane; $t_s$ = one-half the thickness of the doubly-reinforced sheet; $t_a$ = the thickness of the adhesive; and $t_o$ = the thickness of the overlay. In the singly-reinforced case, integration of Eq. (4) between points $b$ and $e$ (Fig. 2b) and substitution into Eq. (2) gives the shear-stiffness coefficient

$$\bar{k}_{sx} = \left( A_s \Big/ \frac{3}{8}\frac{t_s}{G_s} + \frac{t_a}{G_a} + \frac{3}{8}\frac{t_o}{G_o} \right) = \bar{k}_{sy} \tag{6}$$

in which $t_s$ is the total thickness of the singly-reinforced sheet, and the other symbols are defined previously.

The stiffness matrices of the various finite elements, $[k]$ in Eq. (1) and $[k_s]$ in Eq. (3), are superposed to form the stiffness matrix of the entire structure. This is done by adding the stiffness matrix elements that relate displacements to resulting forces for common or adjacent nodal points of adjacent elements. The resulting stiffness matrix of the entire structure $[K]$ relates the external forces applied to the structure $\{F\}$ to the resulting nodal point displacements $\{w\}$ according to the equation

$$\{F\} = [K]\{w\} \tag{7}$$

This equation can be solved for nodal point displacements $\{w\}$ throughout the structure. Then, strains and stresses within the triangular elements can be computed in the usual way.[5] The adhesive shear stresses $\{\tau_s\}$ are obtained by dividing the adhesive shear forces $\{f_s\}$ by the shear area $A_s$; that is

$$\begin{Bmatrix} \tau_{sx} \\ \tau_{sy} \end{Bmatrix} = \frac{1}{A_s} \begin{bmatrix} k_{sx} & 0 \\ 0 & k_{sy} \end{bmatrix} \begin{Bmatrix} u_s \\ v_s \end{Bmatrix} \tag{8}$$

The adhesive shear stress components $\tau_{sx}$ and $\tau_{sy}$ can be added vectorially to give the resultant adhesive shear stress $\tau_s$ at each nodal point within the bonded area.

In the work reported here, weighted average values of nodal point stresses and strains were computed by formulas recommended by Wilson.[6] Nodal point values at material discontinuities were averaged separately for the different materials. These nodal point stresses and strains are the quantities that were contour plotted. The locations of the contour lines were linearly interpolated between pairs of adjacent nodal points.

### Longitudinal Cross-Section Analysis

Figure 3 shows a representative network of triangular, constant strain, finite elements as might be used in a cross-section analysis of a reinforced transverse crack. Symmetry is assumed about the vertical ($z$) axis. Such a network can be used for the cross-section analysis of either singly-reinforced or doubly-reinforced sheet. For the case of a doubly-reinforced sheet, symmetry about the horizontal ($x$) axis is imposed. The crack extends along the $z$ axis for the full thickness of the sheet. The overlay bridges across the crack at the $z$ axis. The actual step taper is approxi-

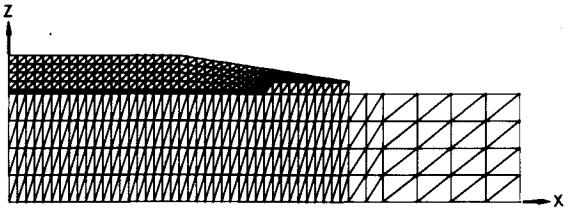


**Fig. 3 Finite element mesh for longitudinal cross-section analysis.**

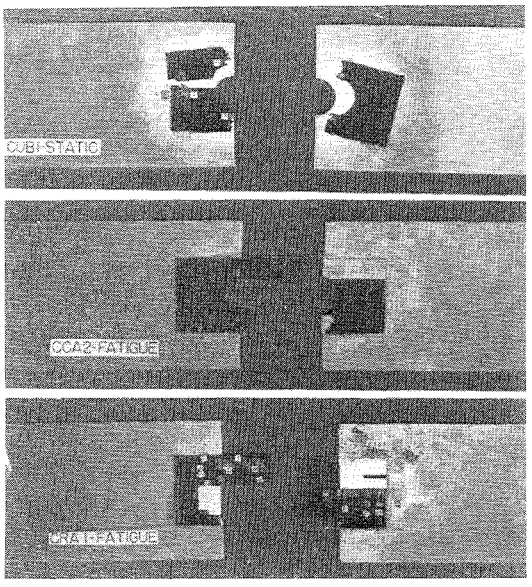


Fig. 4 Reinforced cutout (CUB1), cutout-with-crack (CCA2), and transverse crack (CRA1) specimens.

mated by a uniform taper. External normal loads are assumed to act at the right edge of the sheet.

The orthotropic stress-strain properties of each lamina are first transformed to the axes $x$, $z$; then the effective (weighted average) orthotropic properties are computed for each triangular finite element according to the cross-sectional areas of the separate laminas within the triangular element. No special shear-stiffness elements are used in this analysis. Displacements, nodal-point stresses and strains, and contour lines are computed using the same procedures as in the planform analysis. This analysis can be used to estimate bending effects in singly-reinforced cases, and it can be used to estimate peel stresses in either singly-reinforced or doubly-reinforced cases.

## Comparison with Laboratory Tests

Seventeen double-overlay-reinforced sheet specimens and 9 double-lap joint specimens were tested to failure in tension or low-cycle tension-tension fatigue. Representative specimens of the different configurations, after testing to failure, are shown in Figs. 4 and 5. Combinations of tensile, longitudinal-splitting, debonding, and delamination modes of failure are evident in the figures. No attempt was made to optimize the specimens with respect to structural efficiency. The sheet specimens were 6.0 in. (15.2 cm) wide, and the joint specimens were 1.0 in. (2.5 cm) wide.

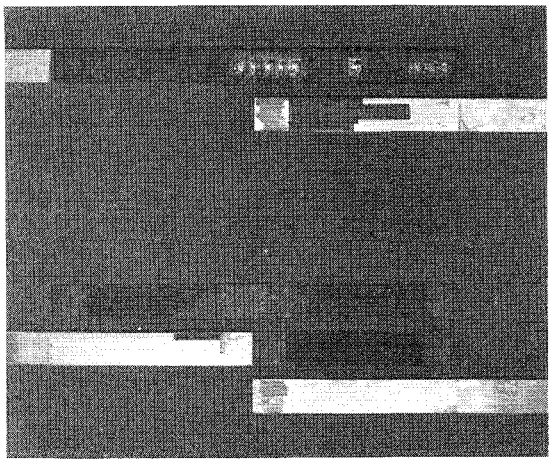

Fig. 5 Double-lap joint specimens.

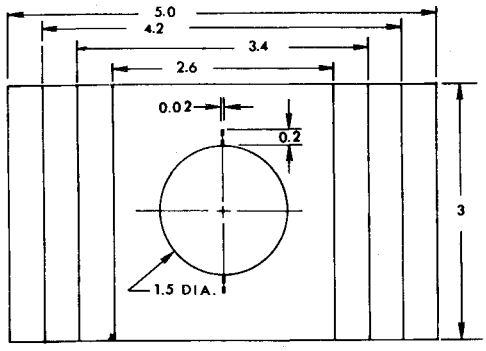


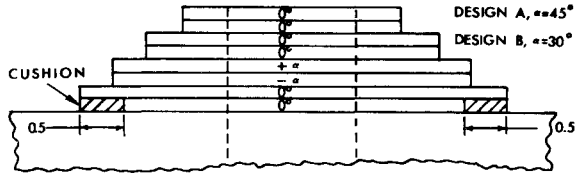


Fig. 6 Composite overlays used to reinforce cutout and cutout-with-crack specimens. Dimensions are in inches (1 in. = 2.54 cm).

The specimens were instrumented with from 4–47 resistance strain gages.

### Specimen Materials

The specimens were made of 0.125-in. (0.32-cm) thick bare aluminum alloy and unidirectional, 0.004-in. (0.1-mm) filament diameter, boron/epoxy preimpregnated material. Three joint specimens were made with 2024-T4 alloy, and the remaining specimens were made with 7075-T6 alloy. The boron/epoxy overlays were laid up and fully cured before being bonded to the aluminum at room temperature.

The following elastic constants for the aluminum alloys were determined by strain measurements on the surfaces of the specimens:

$$E(7075\text{-}T6) = 9.92 \times 10^6 \text{ lbf/in.}^2$$
$$= 68.4 \times 10^9 \text{ N/m}^2$$
$$E(2024\text{-}T4) = 10.40 \times 10^6 \text{ lbf/in.}^2$$
$$= 71.7 \times 10^9 \text{ N/m}^2$$
$$\nu = 0.318$$

The following elastic constants for the boron/epoxy were determined by tensile coupon tests and a thin-tube torsion test:

$$E_{11} = 28.6 \times 10^6 \text{ lbf/in.}^2$$
$$= 197 \times 10^9 \text{ N/m}^2$$

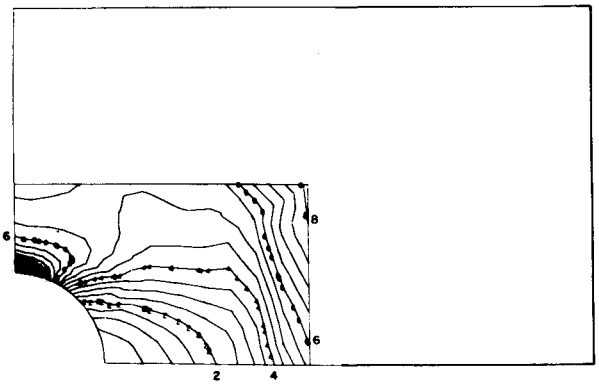


Fig. 7 Contour plot of maximum principal stress in an overlay. Contour interval = 5000 lbf/in.$^2$ = 34.48 × 10$^6$ N/m$^2$.

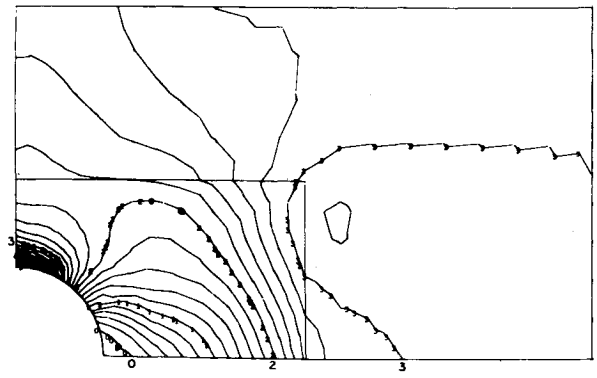

Fig. 8 Contour plot of maximum principal stress in the sheet. Contour interval = 2000 lbf/in.$^2$ = 13.79 × 10$^6$ N/m$^2$.

$$E_{22} = 2.10 \times 10^6 \text{ lbf/in.}^2$$
$$= 14.5 \times 10^9 \text{ N/m}^2$$
$$G_{12} = 0.759 \times 10^6 \text{ lbf/in.}^2$$
$$= 5.22 \times 10^9 \text{ N/m}^2$$
$$\nu_{12} = 0.168$$

Young's modulus for the adhesive, as determined by a compression test of a cylindrical specimen of the adhesive in bulk, was

$$E = 0.27 \times 10^6 \text{ lbf/in.}^2$$
$$= 1.9 \times 10^9 \text{ N/m}^2$$

Poisson's ratio for the adhesive was assumed to be 0.35.

### Reinforced Cutout

Details of the two designs of cutout reinforcement used in the test specimens are given in Fig. 6. The finite element mesh shown in Fig. 1 was used in analyses of these specimens. Figures 7–10 give contour plots of some of the stress and strain fields computed for a Design *B* specimen (CUB1 in Fig. 4) subjected to uniformly distributed tensile stresses of 30,000 lbf/in.$^2$ (206.9 × 10$^6$ N/m$^2$) at each end. The peak normal stresses and strains appear at the edge of the cutout near the *y* axis. The peak *xy* shear strain in the overlay appears at the edge of the cutout, and a ridge of this strain component extends roughly parallel to the *x* axis. The tensile and longitudinal-splitting modes of failure evident in specimen CUB1 (Fig. 4) were present in several cutout specimens and they correlate qualitatively with the contour plots.

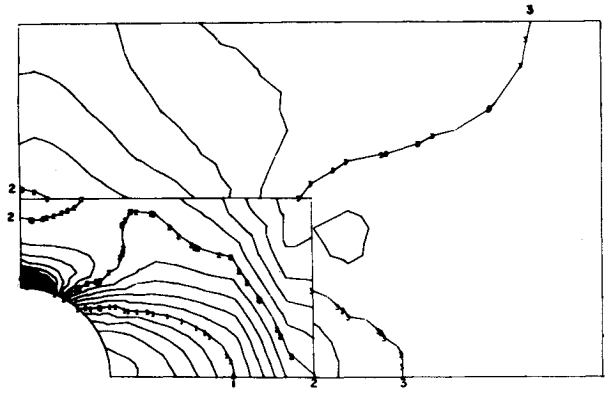

Fig. 9 Contour plot of the *x* component of normal strain in the overlay and in the surrounding sheet. Contour interval = 0.0002.

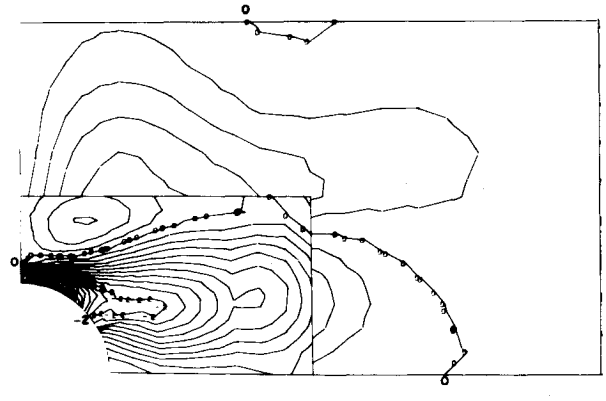

Fig. 10 Contour plot of the *xy* component of shear strain in the overlay and in the surrounding sheet. Contour interval = 0.0002.

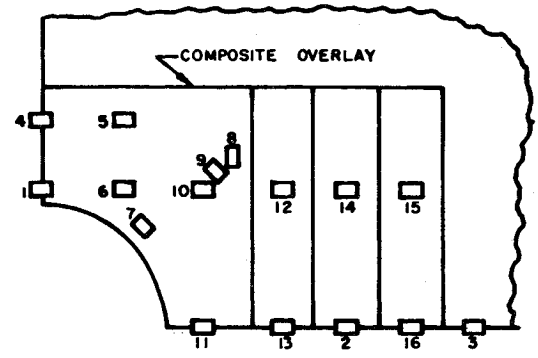


1. 1785(1495, 1101, 1495, 1480)
2. 540(482, 569)
3. 1395(1444, 1386)
4. 1020(1002)
5. 1055(1003)
6. 1200(1238)
7. 875(958)
8. -480(-481)
9. 420(466)
10. 900(859)
11. 95(65)
12. 875(825)
13. 290(259)
14. 1000(982)
15. 1300(1195)
16. 900(788)

Fig. 11 Experimental strains (in parentheses) and analytical strains for a reinforced cutout specimen (CUB1). All values × 10$^6$.

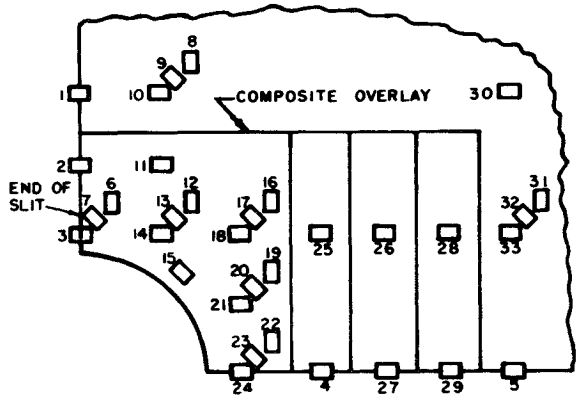


1. 1075(1049, 1164, 1077)
2. 1095(1067, 1060, 1009, 1138)
3. 2275(1674, 1661, 1767, 1895)
4. 325(224, 274, 233, 279)
5. 1400(1365, 1486)
6. -115(-111)
7. 395(498)
8. -350(-354)
9. 245(221)
10. 1140(1149)
11. 1100(1086)
12. -435(-402)
13. 370(428)
14. 1200(1214)
15. 800(757)
16. -500(-457)
17. 435(386)
18. 900(870)
19. -350(-369)
20. 570(617)
21. 300(288)
22. -150(-129)
23. 80(73)
24. 119(61)
25. 910(767)
26. 1045(1048)
27. 610(568)
28. 1300(964)
29. 940(764)
30. 1500(1467)
31. -495(-504)
32. 590(613)
33. 1400(1545)

Fig. 12 Experimental strains (in parentheses) and analytical strains for a reinforced cutout-with-crack specimen (CCA1). All values × 10$^6$.

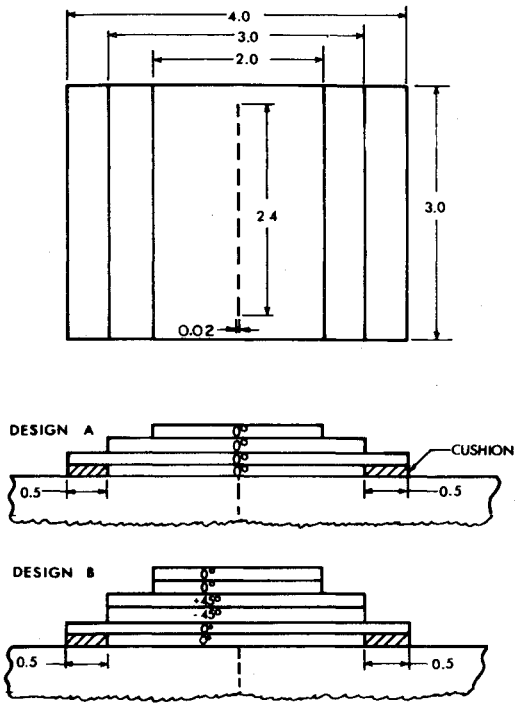


**Fig. 13 Composite overlays used to reinforce transverse crack specimens. Dimensions are in inches (1 in. = 2.54 cm).**

Strains measured on the surface of specimen CUB1 are compared with strains computed by the planform analysis, for an applied tensile load of 11,250 lbf (50,040 N), in Fig. 11. Computed strains are compared with measured values (in parentheses) for the strain gages indicated by the numbered rectangles. Multiple numbers (in parentheses) indicate strain measurements from gages symmetrically located in different quadrants of the specimen.

### Reinforced Cutout-with-Crack

Details of the two designs of cutout reinforcement used in the test specimens are given in Fig. 6. The indicated 0.02-in. (0.5-mm) thick slits were intended to simulate cracks within the sheet radiating away from the cutout edge. The tensile and longitudinal-splitting modes of failure evident in specimen CCA2 (Fig. 4) were also present in other cutout-with-crack specimens and they correlate qualitatively with the planform analysis. Strains measured on the surface of specimen CCA1 are compared with computed strains, for an applied tensile load of 11,250 lbf (50,040 N), in Fig. 12.

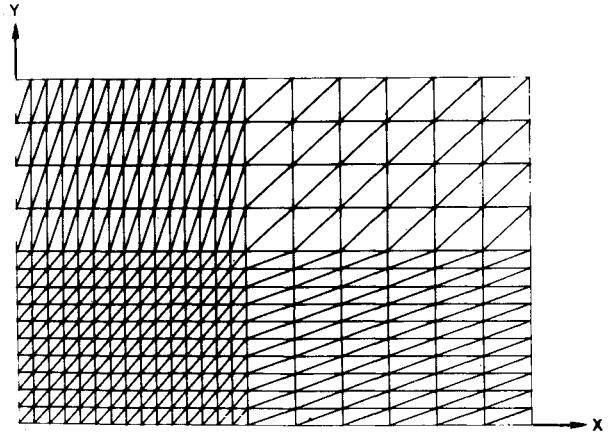


**Fig. 14 Finite element mesh for planform analysis of a reinforced transverse crack.**

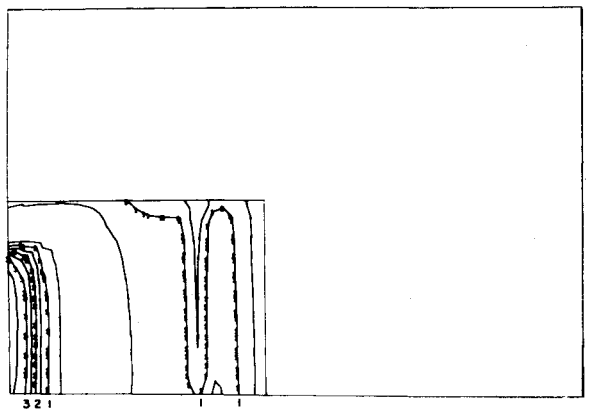


**Fig. 15 Contour plot of resultant adhesive shear stress. Contour interval = 500 lbf/in.$^2$ = 3.45 × 10$^6$ N/m$^2$.**

### Reinforced Transverse Crack

Details of the two designs of overlays used to reinforce the transverse crack specimens are given in Fig. 13. The indicated 0.02-in. (0.5-mm) thick slit was intended to simulate a crack. The finite element mesh shown in Fig. 14 was used in the analysis of these specimens. Figures 15 and 16 give contour plots of 2 of the stress fields computed for a Design B specimen subjected to uniformly distributed tensile stresses of 30,000 lbf/in.$^2$ (206.9 × 10$^6$ N/m$^2$) at each end. The stress contours are roughly parallel to the direction of the transverse crack for a large part of the overlay region. This suggests that the longitudinal cross-section ($x$-$z$ plane) analysis would be useful in the study of reinforced transverse cracks. Strains measured on the surface of specimen CRA1 are compared with computed strains, for an applied tensile load of 11,250 lbf (50,040 N), in Fig. 17.

### Double-Lap Joint

These specimens consisted of 2 pieces of aluminum alloy that were spliced together with 6-ply unidirectional 0° boron/epoxy overlays, 12.0 in. (30.5 cm) long, bonded to each surface. The two specimens shown in Fig. 5 were spliced with uniform-thickness overlays having 1.0-in. (2.5-cm) long, single-ply cushions of unreinforced epoxy at the center and at each end. According to the analyses, the cushions can significantly reduce peak adhesive shear stresses. In these two specimens the cushions apparently precipitated the delamination between the first and second inner plies that is evident in Fig. 5. Strains measured on the surface of one of the specimens (Fig. 5) are compared with strains computed by the longitudinal cross-section analysis, for an applied load of 2500 lbf (11,100 N), in Fig. 18.

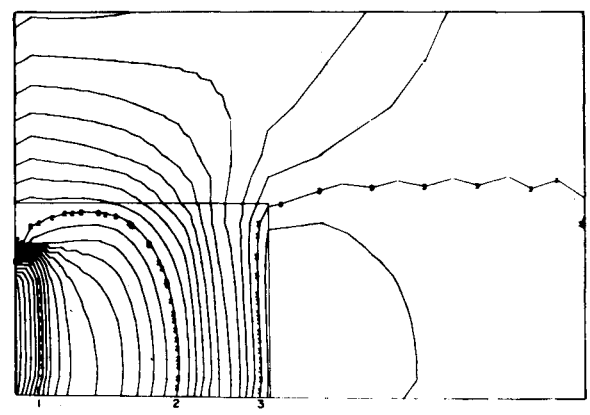


**Fig. 16 Contour plot of maximum principal stress in the sheet. Contour interval = 1000 lbf/in.$^2$ = 6.895 × 10$^6$ N/m$^2$.**

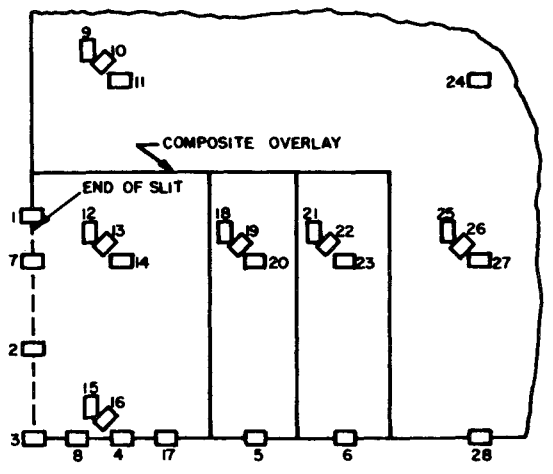


| | | | |
|---|---|---|---|
| 1. | 1050(1086, 1099, 1034) | 15. | -165(-171) |
| 2. | 1300(1388, 1226) | 16. | 329(369) |
| 3. | 1275(1376, 1227) | 17. | 770(747) |
| 4. | 800(825, 792, 807) | 18. | -270(-269) |
| 5. | 840(851, 913) | 19. | 323(350) |
| 6. | 1300(1213, 1223) | 20. | 900(871) |
| 7. | 1250(1341) | 21. | -360(-335) |
| 8. | 925(1016) | 22. | 483(547) |
| 9. | -400(-417) | 23. | 1330(1304) |
| 10. | 445(477) | 24. | 1440(1396) |
| 11. | 1230(1221) | 25. | -465(-474) |
| 12. | -230(-244) | 26. | 630(661) |
| 13. | 306(326) | 27. | 1580(1568) |
| 14. | 875(844) | 28. | 1585(1579) |

**Fig. 17 Experimental strains (in parentheses) and analytical strains for a reinforced transverse-crack specimen (CRA1). All values $\times 10^6$.**

## Other Applications of the Analyses

Adaptations of the planform analysis and the longitudinal cross-section analysis are now being used to study combination joints.§ Combination joints are joints formed by some combination of adhesive bonding or brazing and a more concentrated shear transfer mechanism such as spot-welding, riveting, or bolting. The analysis requires the computation of the effective shear stiffness of the concentrated shear mechanism. This computation is relatively direct for a spotweld. For a fastener, however, it is necessary to consider (analytically and/or empirically) such complications as slip, bearing, and fastener bending.

The analyses could be used to study the repair of holes in metal or composite sheet.[7] In this case the hole is plugged and/or bridged, and most of the load is transferred through the region by a bonded lap shear mechanism.

The planform analysis can directly articulate debonded regions in a larger bonded area. It could similarly be adapted to study such defects as cracks, voids, and enclosures in embedded laminas of laminar material.

## Conclusion

Finite element computer programs have been developed to analyze the reinforcement of cutouts and cracks in metal sheet by adhesively bonded overlays of composite materials. The programs are also suitable for the analysis of adhesively bonded lap joints. The analyses articulate the separate responses of the bonded adherends and the adhesive.

§ This work is being partially supported by U.S. Army, Picatinny Arsenal.

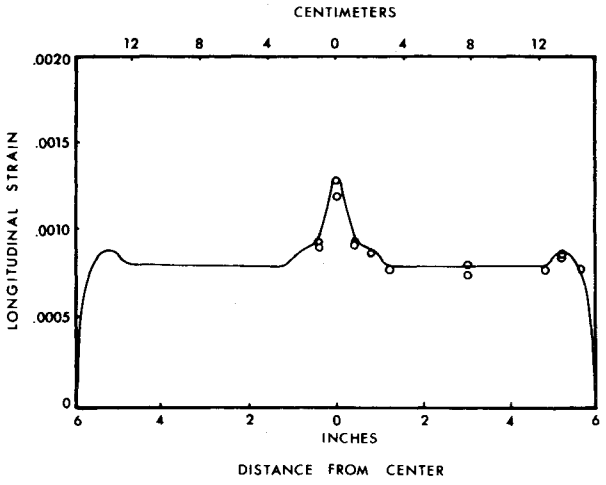


**Fig. 18 Experimental strain (points) and analytical strain for a double-lap joint specimen.**

The computer programs can accommodate the analysis of a broad class of reinforced-cutout, reinforced-crack, and lap-joint configurations. Such special features as cushions, tapers, and debonded regions can be explicitly studied. The computer programs generate the finite element networks from input data in the form of gross dimensions. These characteristics of the programs make them efficient for use in design studies.

A series of laboratory tests was conducted to demonstrate the validity of the analyses. Only a part of the laboratory results has been presented here. More complete analytical and experimental results are given in a separate report.[8] Strains measured on the surfaces of a variety of tests specimens were, for the most part, in good agreement with strains predicted by the analyses. Qualitative correlations between some failure modes and the stresses computed by the analyses were apparent.

## References

[1] Isakson, G. and Levy, A., "Finite Element Analysis of Interlaminar Shear in Fibrous Composites," *Journal of Composite Materials*, Vol. 5, April 1971, pp. 273–276.

[2] Levy, A., Armen, H., and Whiteside, J., "Elastic and Plastic Interlaminar Shear Deformation in Laminated Composites under Generalized Plane Stress," *Proceedings of the Third Conference on Matrix Methods in Structural Mechanics*, Wright-Patterson Air Force Base, Ohio, Oct. 1971.

[3] Barker, R. M., Dana, J. R., and Pryor, C. W. Jr., "Stress Concentrations Near Holes in Laminates," *Journal of the Engineering Mechanics Division, ASCE*, Vol. 100, No. EM3, June 1974, pp. 477–488.

[4] Ashton, J. E., Halpin, J. C., and Petit, P. H., *Primer on Composite Materials: Analysis*, Technomic, Stamford, Conn., 1969, Chap. 2.

[5] Zienkiewicz, O. C., *The Finite Element Method in Engineering Science*, McGraw-Hill, London, 1971.

[6] Wilson, E. L., "Finite Element Analysis of Two-Dimensional Structures," Structures and Materials Research Rept. 63-2, June 1963, University of California, Berkeley, pp. 23–25.

[7] Lubin, G., Dastin, S. J., Mahon, J., and Woodrum, T., "Repair Technology for Boron-Epoxy Structures," *Proceedings of the 27th Annual Tech. Conf.*, Soc. Plastics Industry, Jan. 1972, Sec. 17–B, pp. 1–12.

[8] Mitchell, R. A., Woolley, R. M., and Chwirut, D. J., "Composite-Overlay Reinforcement of Cutouts and Cracks in Metal Sheet," NBSIR 73-201, Feb. 1973, National Bureau of Standards, Washington D.C.